

## Research Article

# Optimization and Prediction of Tribological Behaviour of Al-Fe-Si Alloy-Based Nanograin-Refined Composites Using Taguchi with Response Surface Methodology

S. Balaji,<sup>1</sup> P. Maniarasan,<sup>1</sup> S. V. Alagarsamy,<sup>2</sup> Abdullah M. Alswieleh,<sup>3</sup> V. Mohanavel,<sup>4,5</sup> M. Ravichandran,<sup>5,6</sup> Byong-Hun Jeon,<sup>7</sup> and Haiter Lenin Allasi<sup>8</sup> 

<sup>1</sup>Department of Aeronautical Engineering, Nehru Institute of Engineering and Technology, Coimbatore, 641 105 Tamil Nadu, India

<sup>2</sup>Department of Mechanical Engineering, Mahath Amma Institute of Engineering and Technology, Pudukkottai, 622 101 Tamil Nadu, India

<sup>3</sup>Department of Chemistry, College of Science, King Saud University, Riyadh 11451, Saudi Arabia

<sup>4</sup>Centre for Materials Engineering and Regenerative Medicine, Bharath Institute of Higher Education and Research, Selaiyur, Chennai, Tamil Nadu, 600073, India

<sup>5</sup>Department of Mechanical Engineering, Chandigarh University, Mohali, 140 413 Punjab, India

<sup>6</sup>Department of Mechanical Engineering, University Centre for Research & Development, Chandigarh University, Mohali, 140 413 Punjab, India

<sup>7</sup>Department of Earth Resources & Environmental Engineering, Hanyang University, 222-Wangsimni-ro, Seongdong-gu, Seoul 04763, Republic of Korea

<sup>8</sup>Department of Mechanical Engineering, WOLLO University, Kombolcha Institute of Technology, Kombolcha, Ethiopia

Correspondence should be addressed to Haiter Lenin Allasi; drahlenin@kiot.edu.et

Received 17 February 2022; Revised 30 March 2022; Accepted 4 April 2022; Published 25 May 2022

Academic Editor: Hiwa M. Ahmed

Copyright © 2022 S. Balaji et al. This is an open access article distributed under the Creative Commons Attribution License, which permits unrestricted use, distribution, and reproduction in any medium, provided the original work is properly cited.

Aluminium matrix composites (AMCs) are broadly used to change the monolithic materials in aviation, automotive, and defense industries owing to their superior characteristics such as specific strength with light weight, greater hardness, good wear resistance, and better thermal properties. This novel work was aimed at estimating the specific wear rate (SWR) of zirconium dioxide- ( $ZrO_2$ -) filled AA8011 (Al-Fe-Si alloy) matrix composites. A Taguchi method and response surface methodology (RSM) were used to find out the optimum range of control parameters on SWR of proposed composites. The stir casting technique was used to fabricate the composite specimens with varying proportions (5, 10, and 15 wt.%) of  $ZrO_2$  particle addition. The wear tests were performed as per L27 orthogonal design by using a pin-on-disk apparatus under dry conditions. For this test, four control parameters such as wt.% of  $ZrO_2$ , load, disc velocity, and sliding distance each at three levels were selected. Based on the experimental results, 15 wt.% of  $ZrO_2$ , 29.43 N of load, 0.94 m/s of disc velocity, and 1000 m of sliding distance provide the minimum SWR of the developed composite sample. ANOVA result revealed that the load (49.04%) was the primary dominant factor for affecting the SWR, followed by wt.% of  $ZrO_2$  content (29.24%), respectively. Moreover, scanning electron microscopy (SEM) analysis was performed to study the wear mechanism of worn-out surface of the composite test specimens.

## 1. Introduction

In the past few decades, aluminium and its alloys are essential materials for fabrication of high recital parts in engineering applications like aerospace, automotive, and defense industries due to their excellent characteristics like specific

strength, light weight, high stiffness, good elastic modulus, and better thermal characteristics [1]. Among the many Al series alloys, Al-Fe-Si alloy has emerging material for various engineering structural applications owing to its unique characteristics such as high strength and hardness. However, these alloys have obtained very poor tribological properties.

TABLE 1: Chemical elements of AA8011.

Elements	Fe	Si	Mn	Cu	Zn	Ti	Mg	Cr	Al
Wt.%	1.0	0.9	0.20	0.10	0.10	0.08	0.05	0.05	Remain

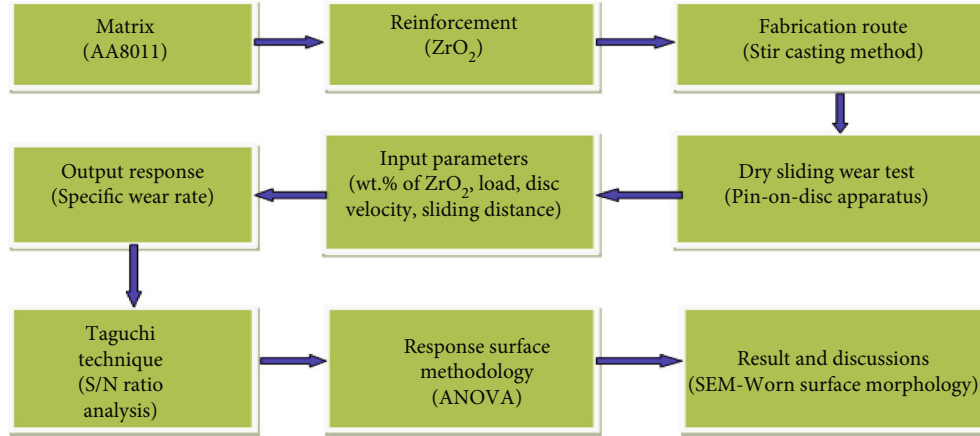


FIGURE 1: The layout of current investigation.

Hence, these alloys are made with self or hard ceramic particulates such as  $ZrO_2$  [2],  $TiC$  [3],  $TiB_2$  [4],  $Al_2O_3$  [5],  $B_4C$  [6, 7],  $ZnO$  [8],  $Si_3N_4$  [9], and  $Gr$  [10] to improve the tribological properties. The development of Al-based composites increases widespread in recent days because of it providing more wear resistance. Stir casting, powder metallurgy, infiltration, compo casting, etc., are commonly employed to develop the AMCs [11]. Among them, stir casting technique is most preferable due to their merits like simple and flexible; more economic and mass production can be achieved [12]. The limitation of the stir casting method is to obtain sufficient wetting of reinforcement particles by molten alloy and to get a homogeneous distribution of the particles and also to reduce the porosity. However, these are prohibited by proper utilization of casting process variables. They [13] fabricated AA7075 composites reinforced with  $TiO_2$  particulates by liquid casting technique, and they reported that the properties of the developed AMCs drastically enhanced due to even allocation of reinforcement. They [14] conducted the wear test of Al- $ZrO_2$  composites under dry conditions and concluded that the wear resistance, improved gradually with an increasing  $ZrO_2$  content. Generally, a variety of factors like load, disc velocity, lubricating medium, and sliding distance are controlling the wear rate of fabricated components. Therefore, selection of optimal parameters is more essential during the wear test. Optimization techniques like the Taguchi method and response surface method are most suitable for prediction of optimum wear control parameter level. The Taguchi method is one of the primary statistical technique which is applied in various areas such as design optimization, parameter selection, and prediction of output responses. It provides a simple, efficient, and systematic approach to optimize the wear control parameters. They [15] optimized the wear parameters of AMCs ( $356/B_4C$ ) using Taguchi technique. They observed that load was a predomi-

TABLE 2: Control parameters and its level.

Symbol	Control parameters	Unit	Level		
			1	2	3
A	% of $ZrO_2$	wt.%	5	10	15
B	Load	N	9.81	19.62	29.43
C	Disc velocity	m/s	0.94	1.88	3.76
D	Sliding distance	m	1000	1500	2000

nant factor trailed by sliding distance with contributions of 35% and 25%, respectively. This work [16] conducted the wear test for AA6062 using a pin-on-disk apparatus under dry conditions. The optimum level of parameters was determined by RSM coupled with desirability analysis. The SEM image of the worn surface reveals that abrasive wear mechanism was occurring. This work [17] optimized the wear control factors such as wt.% of reinforcement, load, sliding distance, and speed on wear resistance of AA7150- $TiO_2$  nanocomposites by employing the Taguchi method. They [18] presented the wear performance of SiC- $ZrO_2$ -filled AMCs, and they reported that a raise in load rises the wear of the fabricated composites. The author [19] considered the wear rate of nanosize of SiC particle-filled AMCs proposed by two-step stir casting route and reported that the dispersion of  $SiC_n$  (60.15%) content was the strongest impact factor, trailed by sliding distance (35.33%), respectively. The worn surface analysis shows that the formation of the oxide layers resists the metal removal from the pin surface, thus resulting in decreasing the wear. They [20] analyzed the tribological performances of  $ZrO_2$ -reinforced Al7068 MMCs produced through liquid metallurgy route. They stated that 12 wt.%  $ZrO_2$  composition addition drastically improves the tribological performances of the matrix alloy. They [21] explored the wear behavior of in situ AA8011- $ZrB_2$  MMCs using Taguchi-Grey analysis, and they

TABLE 3: L27 orthogonal array experimental layout.

Ex. no.	ZrO <sub>2</sub> (wt.%)	Load (N)	Disc velocity (m/s)	Sliding distance (m)	SWR (mm <sup>3</sup> × 10 <sup>-4</sup> /Nm)	S/N ratio (dB)
1	5	9.81	0.94	1000	4.495	-13.055
2	5	9.81	1.88	1500	5.250	-14.403
3	5	9.81	3.76	2000	5.902	-15.420
4	5	19.62	0.94	1500	2.431	-7.716
5	5	19.62	1.88	2000	2.808	-8.968
6	5	19.62	3.76	1000	3.374	-10.563
7	5	29.43	0.94	2000	2.620	-8.366
8	5	29.43	1.88	1000	2.433	-7.723
9	5	29.43	3.76	1500	2.372	-7.502
10	10	9.81	0.94	1500	4.067	-12.185
11	10	9.81	1.88	2000	4.730	-13.497
12	10	9.81	3.76	1000	3.884	-11.786
13	10	19.62	0.94	2000	2.503	-7.969
14	10	19.62	1.88	1000	2.411	-7.644
15	10	19.62	3.76	1500	2.217	-6.915
16	10	29.43	0.94	1000	1.770	-4.959
17	10	29.43	1.88	1500	1.852	-5.353
18	10	29.43	3.76	2000	1.944	-5.774
19	15	9.81	0.94	2000	2.742	-8.761
20	15	9.81	1.88	1000	2.192	-6.817
21	15	9.81	3.76	1500	2.559	-8.161
22	15	19.62	0.94	1000	1.646	-4.329
23	15	19.62	1.88	1500	1.830	-5.249
24	15	19.62	3.76	2000	2.059	-6.273
25	15	29.43	0.94	1500	1.709	-4.655
26	15	29.43	1.88	2000	1.831	-5.254
27	15	29.43	3.76	1000	1.464	-3.311

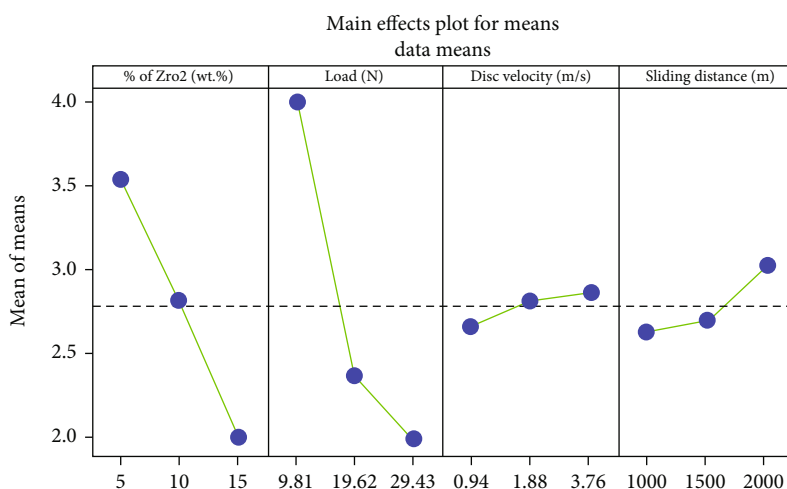


FIGURE 2: Main effect plot for means of SWR.

found that the load and sliding velocity are the most decisive factors among the others. This work [22] predicted the SWR of Al7075 composites incorporated with B<sub>4</sub>C (8wt.%) and fly ash (2wt.%). The RSM was accomplished to create an

empirical model of SWR in terms of various input factors. The worn-out surface shows that the deep plowing grooves and fine debris exist which ensure the presence of plowing mechanism. They [23] studied the wear behavior of LM25

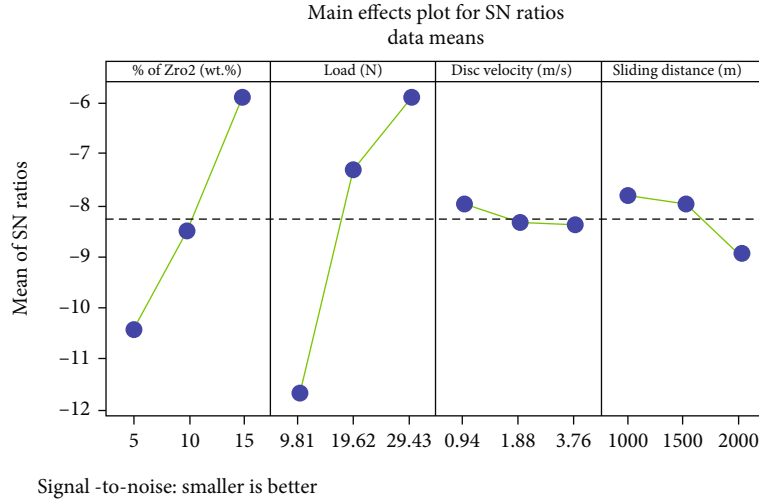


FIGURE 3: Main effect plot for S/N ratios of SWR.

matrix composites reinforced with varying proportions (3, 6, 9, 12, and 15 wt.%) of  $ZrO_2$  particles. They reported that the WR decreases with an increase in the wt.% of  $ZrO_2$  content.

From the detailed literatures, we had observed that the most research work has been studied on AA8011 with different reinforcements such as  $B_4C$ ,  $Al_2O_3$ , SiC, TiC,  $TiB_2$ ,  $Si_3N_4$ , and graphite, but none of them attempted for AA8011 with  $ZrO_2$  as reinforcement via stir casting route. Hence, the present work was aimed at analyzing the SWR of  $ZrO_2$ -filled AA8011 matrix composites developed through stir casting route. An optimization technique such as the Taguchi method and RSM has been applied to find out the optimum conditions of factors on SWR of the fabricated composites.

## 2. Materials and Methods

In the current study, the matrix constituent was chosen as AA8011 (Al-Fe-Si alloy) received from Coimbatore Metal Mart, Coimbatore, India. Recently, AA8011-containing Al-Fe-Si alloy has emerging material in modern engineering applications such as aerospace, automotive, and defense industries where enhanced strength, hardness, and good wear resistance materials are enormously required. Table 1 provided the weight fraction of chemical elements present in the matrix alloy. Similarly, the reinforcement was used as zirconia ( $ZrO_2$ ) particulates with a particle size of  $10 \mu m$  received from LOBA Chemie, Mumbai, India. It has a density of  $5.68 g/cm^3$ , hardness of  $1350 kg/mm^2$ , Young's modulus of 250 GPa, and thermal conductivity of  $2.7 W/m.K$ , respectively. The stir casting technique adopted the production of AA8011 matrix composites by adding different weight fractions (5 wt.%, 10 wt.%, and 15 wt.%) of  $ZrO_2$  particles. The layout of current investigation is illustrated in Figure 1.

Primarily, the required amount of AA8011 rod was stored into the crucible, and it was placed in the electric furnace. The furnace temperature was maintained at  $750^\circ C$ , till the entire alloy was melted. At the same time, the different weight percentages such as 5 wt.%, 10 wt.%, and 15 wt.% of

TABLE 4: Means table for SWR.

Level	A	B	C	D
1	3.521	3.980	2.665	2.630
2	2.820	2.364	2.815	2.699
3	2.004	1.999	2.864	3.015
Delta	1.517	1.981	0.199	0.386
Rank	2	1	4	3

TABLE 5: S/N ratios table for SWR.

Level	A	B	C	D
1	-10.413	-11.565	-7.999*	-7.798*
2	-8.454	-7.292	-8.323	-8.016
3	-5.868*	-5.877*	-8.412	-8.920
Delta	4.545	5.688	0.412	1.122
Rank	2	1	4	3

\*Optimum level.

$ZrO_2$  particles were preheated at  $300^\circ C$  [12] to promote the dry condition and proper wettability with the molten metal. After that, the  $ZrO_2$  particles were slowly fed into the slurry of molten alloy. Meanwhile, the composite slurry was stirred at a speed of 300 rpm about 10 min [13]. Then, the slurry was poured into the mould, and it was permitted to solidify at normal air temperature. After solidification, the composites were taken out from the mould, and the required test specimens were prepared.

After getting the composite specimen, the wear test was executed according to ASTM G-99 standard by TR-20 DUCOM pin-on-disk tribometer. The wear test pins' size of  $10 mm \times 10 mm \times 30 mm$  was prepared by wire cut EDM. During the wear test, the test pins were pushed on the EN-31 steel counter disc with 60 HR<sub>C</sub> hardness. To achieve the clean surface, the test specimen and the counter disc were polished using fine emery sheet and also cleaned by the

TABLE 6: ANOVA table for SWR.

Source	Adj SS	Dof	Adj MS	F-value	P value
Model	34.84	14	2.49	21.27	<0.0001
A-% of ZrO <sub>2</sub>	10.60	1	10.60	90.62	<0.0001
B-load	17.78	1	17.78	151.97	<0.0001
C-disc velocity	0.1784	1	0.1784	1.52	0.2405
D-sliding distance	0.6495	1	0.6495	5.55	0.0363
AB	2.68	1	2.68	22.94	0.0004
AC	0.2506	1	0.2506	2.14	0.1690
AD	0.0227	1	0.0227	0.1937	0.6677
BC	0.1555	1	0.1555	1.33	0.2714
BD	0.2591	1	0.2591	2.21	0.1625
CD	0.0012	1	0.0012	0.0099	0.9223
A <sup>2</sup>	0.0200	1	0.0200	0.1709	0.6866
B <sup>2</sup>	2.35	1	2.35	20.06	0.0008
C <sup>2</sup>	0.0409	1	0.0409	0.3496	0.5653
D <sup>2</sup>	0.0924	1	0.0924	0.7900	0.3916
Residual	1.40	12	0.1170		
Cor total	36.25	26		R <sup>2</sup>	0.9613
Std. Dev.	0.3420			Adjusted R <sup>2</sup>	0.9161
Mean	2.78			Predicted R <sup>2</sup>	0.7769
C.V. %	12.30			Adeq precision	17.6566

acetone solution. Usually, there are many control parameters involved to conduct the wear test. Based on the earlier studies [13], we have considered four parameters with three levels such as wt.% of ZrO<sub>2</sub> (A), load (B), disc velocity (C), and sliding distance (D), respectively. Based on the parameters and its levels (Table 2), Taguchi L<sub>27</sub> orthogonal design was formulated to perform the wear tests. After the tests, the SWR of tested composite specimens is determined by using

$$\text{SWR}(\text{mm}^3/\text{Nm}) = \frac{\Delta m/\rho}{L \times D}, \quad (1)$$

where  $\Delta m$  is the mass loss of test pin (g),  $\rho$  is the density of the fabricated composite (g/mm<sup>3</sup>),  $L$  is the load (N), and  $D$  is the sliding distance (m). The estimated SWR for each experiment is provided in Table 3.

### 3. Optimization Methodologies

**3.1. Taguchi Method.** The Taguchi method is a reliable statistical approach which can be employed to find out the permissible range of parameter conditions with minimum experimental trials performed. The intend of this method is used to make high-quality product with minimum cost [24]. For applying this method, suitable orthogonal array design is formulated based on the quantity of input factors and its levels concerned. Notably, three arithmetic S/N ratio equations can be used to determine the response such as smaller is better, nominal is best, and larger is better, respectively [25]. Here, the objective of this study is to identify the

optimal control factors on SWR while dry sliding process of AA8011-ZrO<sub>2</sub> composites. To compute the S/N ratio for the SWR, smaller the better arithmetic S/N ratio equation can be used and it was provided in

$$\text{S/Nratio} = -10 \log_{10}(1/n) \sum_{k=1}^n Y_{ij}^2, \quad (2)$$

where  $n$  is the no. of trials and  $Y_{ij}$  is the response, where  $i = 1, 2, 3 \dots n$  and  $j = 1, 2, 3 \dots k$ . The calculated S/N ratios for the SWR are given in Table 3.

**3.2. Response Surface Method.** RSM is a powerful and advanced mathematical tool. The main goal of this method is to determine the impact of independent factors on the dependent responses clearly represented by theoretically developed model [26]. In this study, we had employed to predict the SWR and how it is dominated by the independent control factors including wt.% ZrO<sub>2</sub> (A), load (B), disc velocity (C), and sliding distance (D), respectively, by using the “design expert version 12” software, to create an empirical model of SWR in terms of control parameters. To explicate the mathematical appropriate relation between the input factors and SWR, the second-order polynomial regression equation was proposed.

$$Y = \beta_0 + \sum_{i=1}^k \beta_i X_i + \sum_{i=1}^k \beta_{ii} X_i^2 + \sum_{i<j}^k \beta_{ij} X_i X_j + \varepsilon. \quad (3)$$

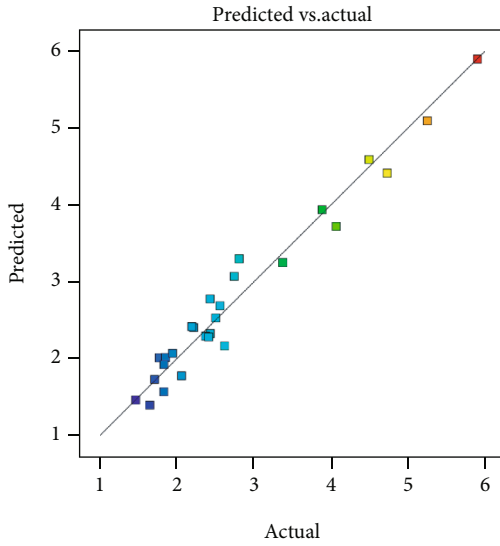


FIGURE 4: Predicted vs. actual plot for SWR.

Here,  $\beta_0$  is constant,  $\beta_i$  is the linear terms,  $\beta_{ii}$  is the quadratic terms,  $\beta_{ij}$  is the interaction terms, and  $X_i$  and  $X_j$  are the levels of input parameters, respectively.

#### 4. Results and Discussion

**4.1. S/N Ratio Analysis.** Figures 2 and 3 reveals the main effect plots for mean and S/N ratio on the SWR with each level of control parameters, namely, wt.% of  $ZrO_2$ , load, disc velocity, and sliding distance. In Figure 2, it is seen that the SWR is gradually decreased with an increasing trend of  $ZrO_2$  content. The reason is that the inclusion of ceramic ( $ZrO_2$ ) particulates improved the hardness of the fabricated composites, which result in reduced the SWR. From Figure 3, it can be proved that the higher S/N ratio is nearer to the optimum conditions. Hence, the less SWR is produced at the optimum level parameters  $A_3B_3C_1D_1$ , represented as wt.% of  $ZrO_2$  at 15 wt.%, load at 29.43 N, disc velocity of 0.94 m/s, and sliding distance at 1000 m. Tables 4 and 5 depicted the response table for means and S/N ratio of SWR. It was revealed that the order of impact parameters on response is represented as rank 1, 2, ..., etc. Normally, the rank 1 is assigned as most significant parameter followed by others. Based on Tables 4 and 5, it can be understood that the load has been identified as rank 1 which is more influencing parameter on SWR, subsequently by wt.% of  $ZrO_2$ , sliding distance, and disc velocity, respectively. The SWR is directly proportional to the load applied, which is obeyed by Archard's law. Hence, the SWR increases with increasing applied load due to more contact pressure between the surfaces. The similar observations were previously reported [27].

**4.2. Analysis of Variance (ANOVA).** ANOVA is a collection of statistical approach used to decide the noteworthy parameters on the responses under the group of process parameters [28]. The purpose of the current investigation is to

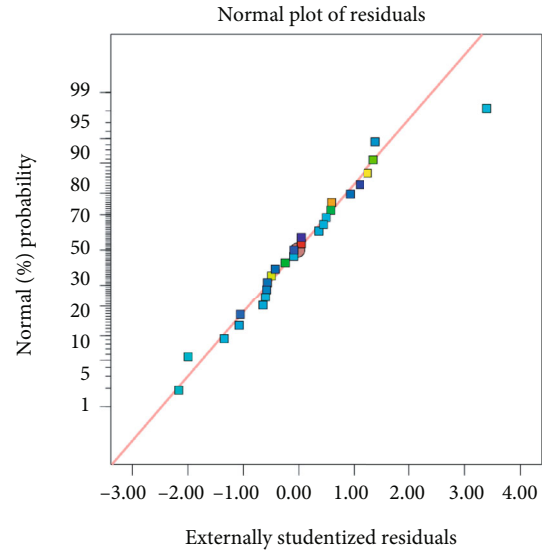


FIGURE 5: Normal probability plot for SWR.

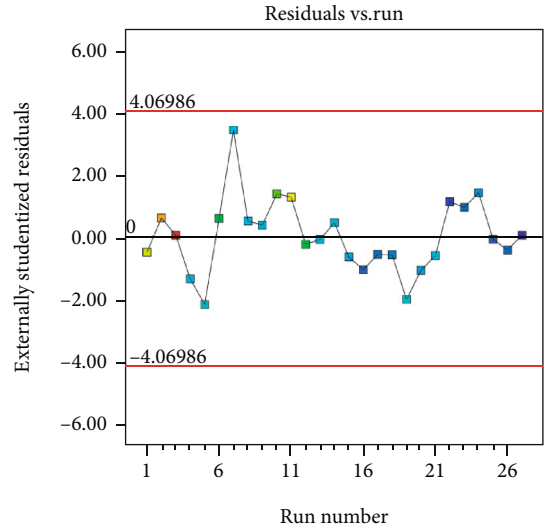


FIGURE 6: Residual vs. run plot for SWR.

identify the impact of control parameters including wt.%  $ZrO_2$  (A), load (B), disc velocity (C), and sliding distance (D) on SWR during dry sliding wear test. ANOVA result of SWR is presented in Table 6. In order to find the noteworthy effect of parameters on SWR, the  $F$ -ratio and  $P$  value (Table 6) are considered at 95% CI and 5% significant level. The  $F$ -value of 21.27 indicates that the developed empirical model is significant, as seen in Table 5. Similarly, the developed model terms are significant which ensured by the  $P$  value ( $<0.0001$ ). It has also been found that the terms A, B, D, AB, and  $B^2$  are considered as the important (most dominant) factors on the SWR. Usually, the  $R^2$  is used to determine the fitness of the empirical model. For current analysis,  $R^2$  value is 0.9613 and adjusted  $R^2$  value is 0.9161 which shows the greater significance of the model. Hence, there is also a well concurrence between the predicted and the adjusted  $R^2$  value.

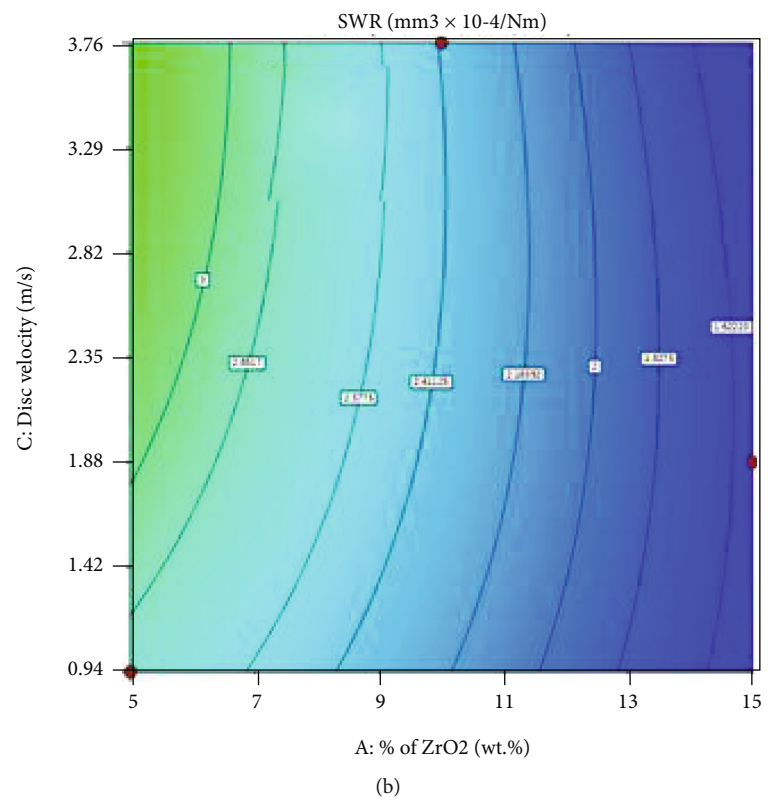
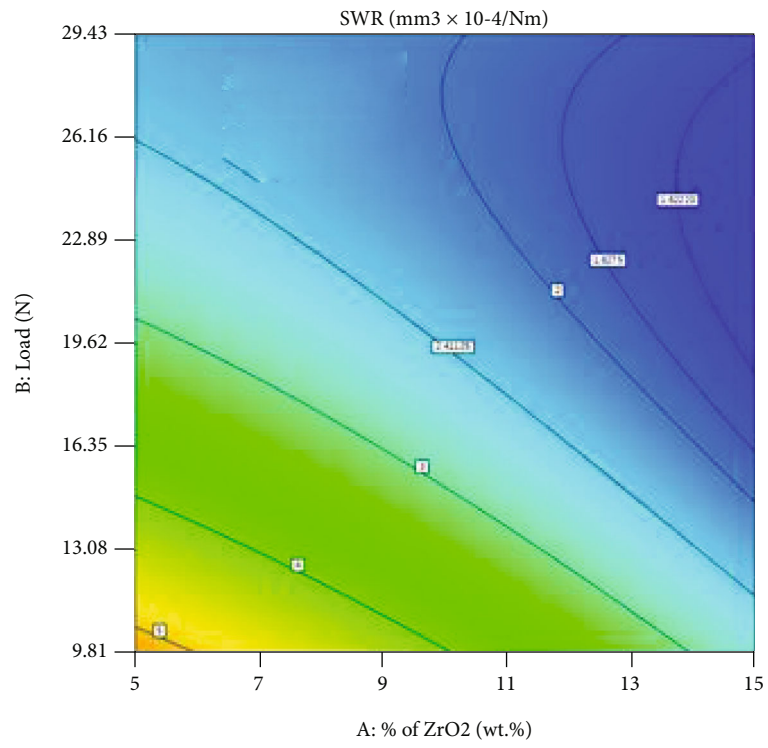
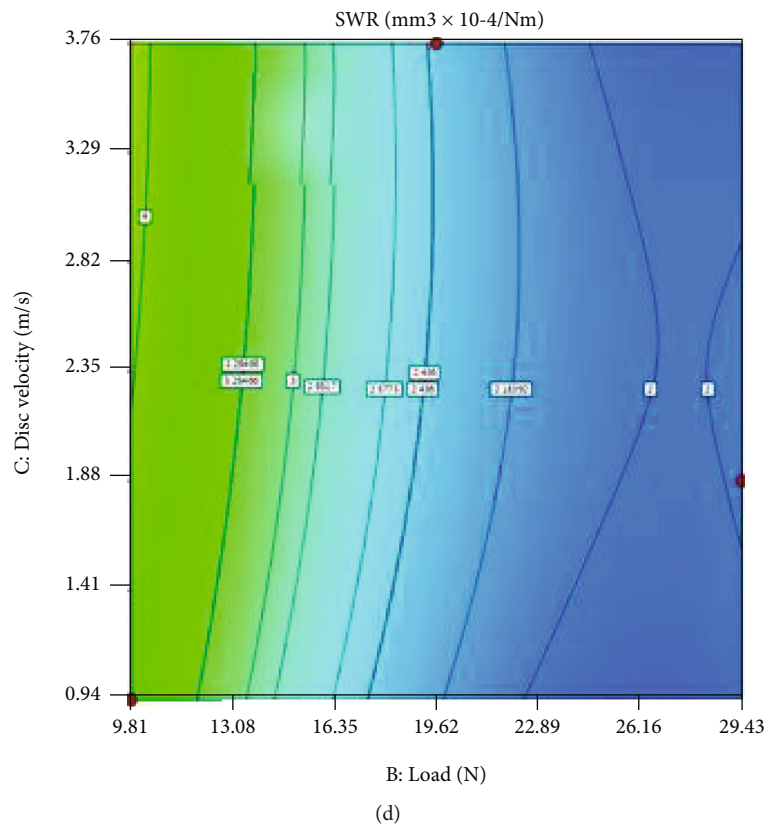
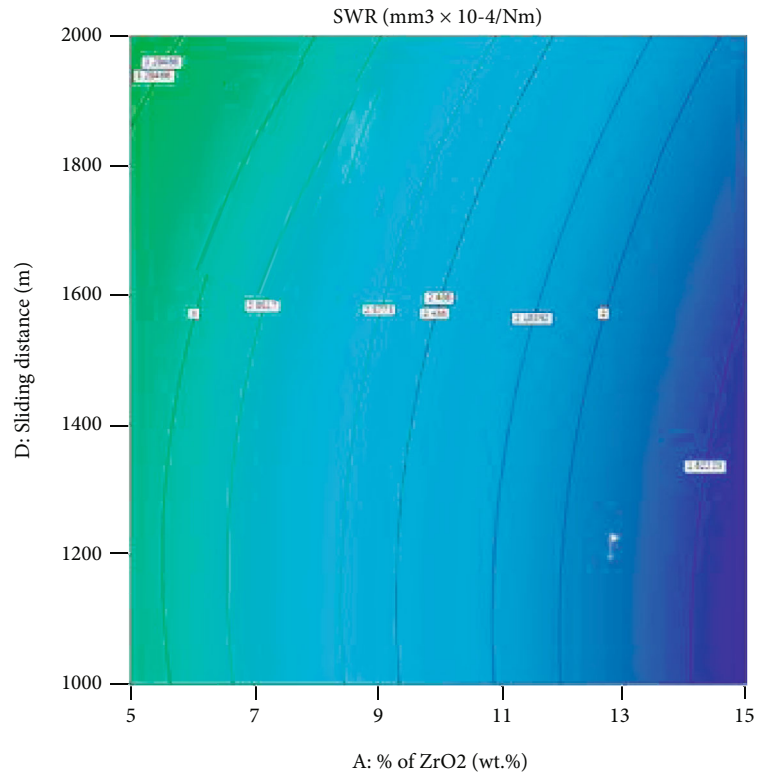


FIGURE 7: Continued.





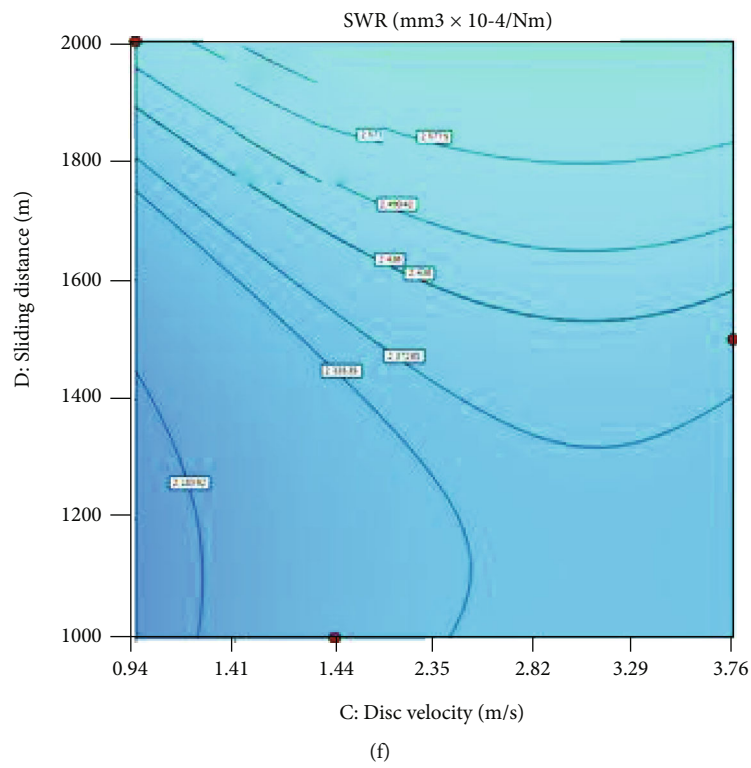
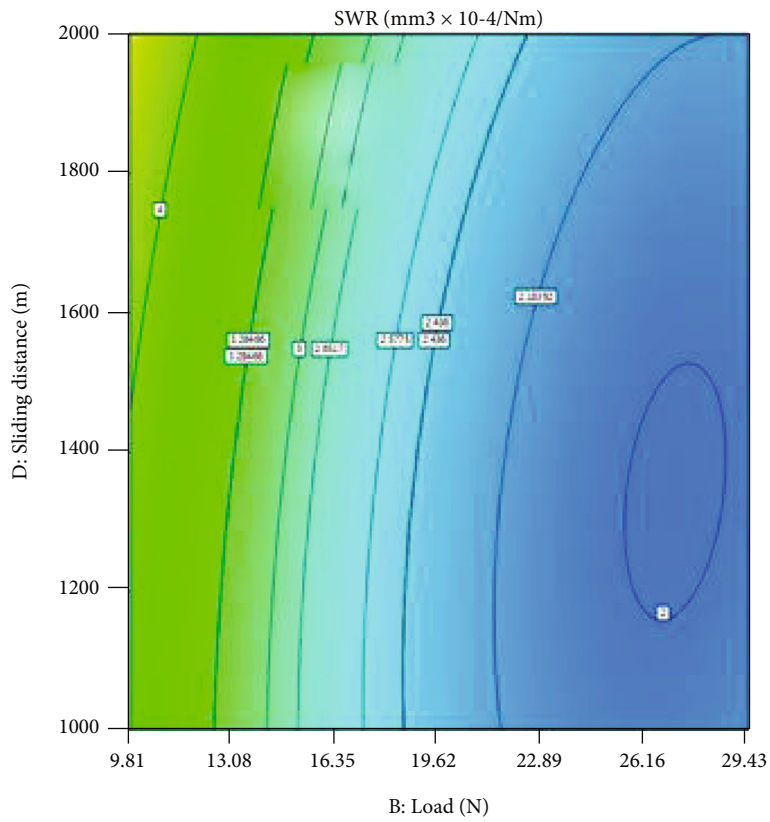


FIGURE 7: (a-f) Contour plots for SWR with respect to control parameters.

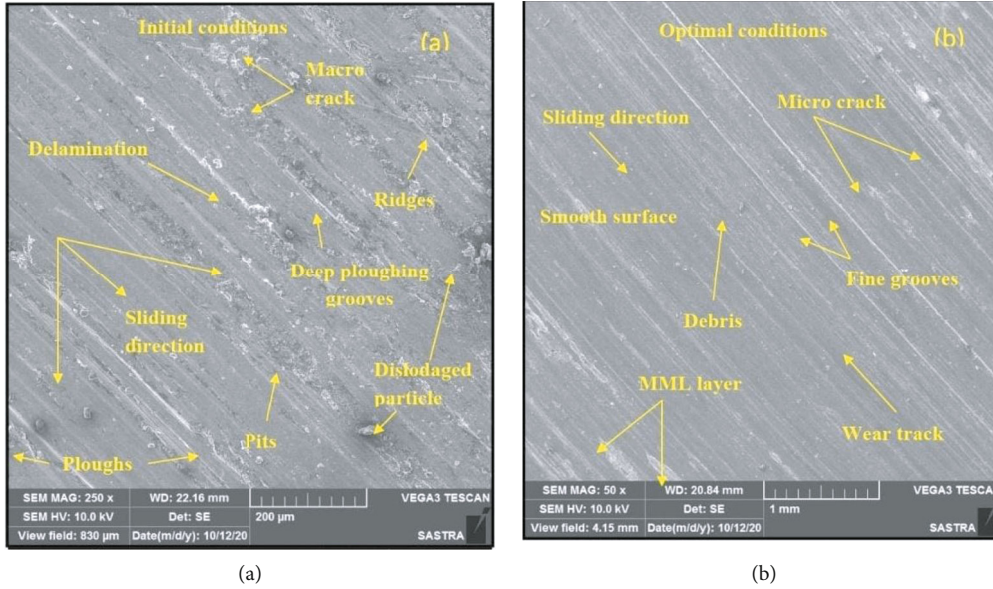


FIGURE 8: SEM images of the worn-out surface (a) at initial conditions and (b) at optimal conditions.

The mathematical relations for the SWR in terms of coded and actual factors are given in

$$\begin{aligned} \text{SWR} = & +2.40 - 0.7745A - 1.00B + 0.0996C + 0.1917D \\ & + 0.4794AB - 0.1438AC + 0.0441AD - 0.1133BC \\ & - 0.1489BD - 0.0098CD - 0.0577A^2 + 0.6254B^2 \\ & + 0.0946C^2 + 0.1241D^2, \end{aligned} \quad (4)$$

$$\begin{aligned} \text{SWR} = & +8.718 - 0.2789A - 0.3901B + 0.6798C \\ & - 0.0006D + 0.0097AB + 0.0204AC \\ & + 0.000018AD - 0.008192BC - 0.000030BD \\ & - 0.000014CD - 0.002309A^2 + 0.006499B^2 \\ & - 0.047575C^2 + 4.964E^{-7}D^2. \end{aligned} \quad (5)$$

Figure 4 displays the predicted and actual values of SWR. It clearly understood that the predicted values are reasonably closer to the experimental values. Figure 5 shows the probability vs. externally studentized residual plot of the SWR. It can be ensured that the residuals are evenly located along a straight line, which confirms that the developed model is fitted. The externally studentized residual with experiment order is shown in Figure 6. From the plot, the experiment number 7 provided the high residual value among the others.

**4.3. Interaction Effect of Parameters on SWR.** Figure 7 illustrates the 2D surface plots for SWR with related to the control parameters. The main purpose of surface plot is used to reveal the interaction effect of parameters on the response. Figures 7(a)–7(c) illustrate the interaction of reinforcement on SWR of developed composites with respect to other parameters like load (B), disc velocity (C), and sliding distance (D). It can be revealed that the SWR gradually increases with increasing the weight.% of ZrO<sub>2</sub> particles.

By considering the load (B), SWR is less for AA8011-15 wt.% of ZrO<sub>2</sub> composite with maximum load condition. The middle level of disc velocity (C) produces low SWR for 15 wt.% of ZrO<sub>2</sub> composite. By considering the sliding distance (D), the higher SWR is produced at higher levels of sliding distance (2000 m) with low weight.% of ZrO<sub>2</sub> content. Figures 7(d) and 7(e) show the interaction of load (B) with disc velocity (C) and sliding distance (D) on SWR. SWR increases with an increasing trend of disc velocity at low level of load (9.81 N). However, the low SWR of  $2 \text{ mm}^3 \times 10^{-4} / \text{Nm}$  is obtained at 29.43 N of load with the middle level of disc velocity. From Figure 7(e), it can be observed that the high SWR of  $4 \text{ mm}^3 \times 10^{-4} / \text{Nm}$  is produced at a maximum sliding distance of 2000 m with initial load of 9.81 N. The effects of disc velocity (C) and sliding distance (D) on SWR is shown in Figure 7 (f). It can be clearly revealed that the SWR steadily increases with an increase in the sliding distance at middle level of disc velocity 1.88 m/s. But, the less SWR  $2.18 \text{ mm}^3 \times 10^{-4} / \text{Nm}$  is attained at 0.94 m/s disc velocity and 1000 m sliding distance, respectively.

**4.4. Worn Surface Morphology.** The SEM morphology of the worn-out surface of developed AA8011-ZrO<sub>2</sub> composite specimens tested at various conditions of control parameters is illustrated in Figures 8(a) and 8(b). From the figure, the presence of mechanisms in the worn surfaces was exactly noticed.

Figure 8(a) depicts the worn-out surface of the initial test conditions including 5 wt.% of ZrO<sub>2</sub>-filled composite at a load of 9.81 N, disc velocity of 0.94 m/s, and sliding distance of 1000 m, respectively. It shows the presence of deep ploughing grooves, delamination, some pits, and macrocrack on the worn-out surface. The asperities of the counter disc generated deep ploughing grooves while sliding, resulting in the formation of ridges. The dislodged particles existence in some region due to the repetitive sliding action and also

some debris removed from the ridges. Due to the removal of reinforcement ( $ZrO_2$ ) particles, some pits are formed in the worn-out surface. This causes the abrasive mechanism involved. The worn-out surface of the optimal test conditions of 15 wt.% of  $ZrO_2$ -dispersed composite at a load of 29.43 N, disc velocity of 0.94 m/s, and sliding distance of 1000 m is shown in Figure 8(b). It obviously revealed the presence of the smooth surface as well as fine grooves on the worn-out surface. The reason is behind that is that the dispersion of higher amount of  $ZrO_2$  (15 wt.%) particles improves the surface hardness among the other composites, thus will reduce the SWR. Due to higher load (29.43 N) conditions, the microcrack exists in a few regions on the surface. However, the mechanical mixed layer (MML) is formed due to transfer of materials between the counterpart and pin surface which causes reduced the SWR.

## 5. Conclusions

This work investigated the effects of control parameters on SWR of zirconia- ( $ZrO_2$ -) filled AA8011 composites under dry sliding conditions. The given observations were obtained in this study:

- (i) The various weight fractions (5, 10, and 15 wt.%) of  $ZrO_2$  particle were incorporated with AA8011 matrix composites through stir casting route. A pin-on-disk machine was used to conduct the wear tests under dry conditions
- (ii) A Taguchi technique was applied to identify the optimal control parameters on SWR of proposed composites. Based on the main effect plot, the less SWR is obtained at 15 wt.% of  $ZrO_2$ , 29.43 N of load, 0.94 m/s of disc velocity, and 1000 m of sliding distance
- (iii) RSM-based ANOVA result revealed that the load has been considered as the more influencing parameter on SWR, followed by wt.% of  $ZrO_2$  content with percentage contributions of 49% and 29.24%, respectively
- (iv) SWR drastically minimizes when there is an increasing trend of  $ZrO_2$  particles within the matrix alloy. The reason is behind that is that the inclusions of ceramic content improved the hardness, thus reducing the SWR of the developed composite
- (v) The SEM micrograph of the worn-out surface reveals the presence of deep grooves, plugs, and cracks on the surface of the initial parametric conditions. However, at optimal parametric conditions, the fine grooves and smooth surface are formed due to higher amount (15 wt.%) of  $ZrO_2$  addition that creates the MML layer, thus reducing the SWR
- (vi) In the future, other optimization techniques such as fuzzy logic and artificial neural network and machine learning approaches can be used to predict the SWR of the developed composites

## Data Availability

The data used to support the findings of this study are included within the article. Further data or information is available from the corresponding author upon request.

## Conflicts of Interest

The authors declare that there are no conflicts of interest regarding the publication of this paper.

## Acknowledgments

The authors appreciate the support from the Wollo University, Kombolcha Institute of Technology, Ethiopia, for the research and preparation of the manuscript. The authors would like to acknowledge the Researchers Supporting Project number (RSP-2021/238), King Saud University, Riyadh, Saudi Arabia.

## References

- [1] V. Mohanavel, K. Rajan, and M. Ravichandran, "Synthesis, characterization and properties of stir cast AA6351-aluminium nitride (AlN) composites," *Journal of Materials Research*, vol. 31, no. 24, pp. 3824–3831, 2016.
- [2] H. Ghandvar, S. Farahany, M. H. Idris, and M. Daroonparvar, "Dry sliding wear behavior of A356-ZrO<sub>2</sub> metal matrix composite," *Advanced Materials Research*, vol. 1125, pp. 116–120, 2015.
- [3] S. Baskaran, V. Anandkrishnan, and M. Duraiselvam, "Investigations on dry sliding wear behavior of in situ casted AA7075-TiC metal matrix composites by using Taguchi technique," *Materials and Design*, vol. 60, pp. 184–192, 2014.
- [4] V. Mohanavel, "Mechanical and microstructural characterization of AA7178-TiB<sub>2</sub> composites," *Materials Testing*, vol. 62, no. 2, pp. 146–150, 2020.
- [5] S. Sakthivelu, P. P. Sethusundaram, M. Ravichandran, and M. Meignanamoorthy, "Experimental investigation and analysis of properties and dry sliding wear behavior of Al-Fe-Si alloy matrix composites," *Silicon*, vol. 13, pp. 1285–1294, 2021.
- [6] J. A. Jeffrey, S. S. Kumar, V. A. Roseline, A. L. Mary, and D. Santhosh, "Contriving and assessment of magnesium alloy composites augmented with boron carbide VIA liquid metallurgy route," *Materials Science Forum*, vol. 1048, pp. 3–8, 2022.
- [7] R. Suresh, "Comparative study on dry sliding wear behavior of mono (Al<sub>2219</sub>/B<sub>4</sub>C) and hybrid (Al<sub>2219</sub>/B<sub>4</sub>C/Gr) metal matrix composites using statistical technique," *Journal of the Mechanical Behavior of Materials*, vol. 29, no. 1, pp. 57–68, 2020.
- [8] M. I. U. Haq and A. Anand, "Dry sliding friction and wear behavior of AA7075-Si<sub>3</sub>N<sub>4</sub> composite," *Silicon*, vol. 10, pp. 1819–1829, 2018.
- [9] S. V. Alagarsamy, R. Balasundaram, M. Ravichandran, V. Mohanavel, A. Karthick, and S. S. Devi, "Taguchi approach and decision tree algorithm for prediction of wear rate in zinc oxide-filled AA7075 matrix composites," *Surface Topography*, vol. 9, pp. 1–15, 2021.
- [10] N. Radhika, R. Subramanian, S. V. Prasat, and B. Anandavel, "Dry sliding wear behaviour of aluminium/alumina/graphite

- hybrid metal matrix composites," *Industrial Lubrication and Tribology*, vol. 64, pp. 356–366, 2021.
- [11] B. S. Yigezu, P. K. Jha, and M. M. Mahapatra, "The key attributes of synthesizing ceramic particulate reinforced Al-based matrix composites through stir casting process: a review," *Materials and Manufacturing Processes*, vol. 28, pp. 969–979, 2013.
- [12] S. Balaji, P. Maniarsan, S. V. Alagarsamy, and P. Raveendran, "Dry sliding wear behaviour of aluminium metal matrix composite using response surface methodology," *Materials Today: Proceedings*, vol. 2021, 2021.
- [13] S. V. Alagarsamy and M. Ravichandran, "Parametric studies on dry sliding wear behaviour of Al-7075 alloy matrix composite using S/N ratio and ANOVA analysis," *Materials Research Express*, vol. 7, pp. 1–17, 2020.
- [14] M. Ramachandra, A. Abhishek, P. Siddeshwar, and V. Bharathi, "Hardness and wear resistance of ZrO<sub>2</sub> nano particle reinforced Al nano composites produced by powder metallurgy," *Procedia Materials Science*, vol. 10, pp. 212–219, 2015.
- [15] J. Udaya Prakash, S. Jebarose Juliyana, M. Saleem, and T. V. Moorthy, "Optimization of dry sliding wear parameters of aluminium matrix composites (356/B<sub>4</sub>C) using Taguchi technique," *International Journal of Ambient Energy*, vol. 42, no. 2, pp. 140–142, 2018.
- [16] K. Gajalakshmi, N. Senthilkumar, and B. Prabu, "Multi-response optimization of dry sliding wear parameters of AA6026 using hybrid gray relational analysis coupled with response surface method," *Measurement and Control*, vol. 52, no. 5–6, pp. 540–553, 2019.
- [17] P. Madhukar, N. Selvaraj, V. Mishra, and C. S. P. Rao, "Optimization of wear parameters of AA7150-TiC nanocomposites by Taguchi technique," *Numerical Optimization in Engineering and Sciences*, vol. 979, pp. 543–550, 2020.
- [18] A. G. Joshi, M. Manjaiah, S. Basavarajappa, and R. Suresh, "Wear performance optimization of SiC-Gr reinforced Al hybrid metal matrix composites using integrated regression-antlion algorithm," *Silicon*, vol. 13, no. 11, pp. 3941–3951, 2020.
- [19] M. T. Alam, S. Arif, A. H. Ansari, and M. N. Alam, "Optimization of wear behaviour using Taguchi and ANN of fabricated aluminium matrix nanocomposites by two-step stir casting," *Materials Research Express*, vol. 6, no. 6, pp. 1–10, 2019.
- [20] M. Madhusudhan and K. Mahesha, "Taguchi based validation of wear prediction for Zirconium dioxide particulate reinforced aluminium 7068 composites," *International Journal of Metallurgy and Alloys*, vol. 4, no. 1, pp. 37–50, 2018.
- [21] B. M. MuthamizhSelvan, V. Anandkrishnan, M. Duraiselvam, R. Venkatraman, and S. Sathish, "Multi objective optimization of wear behaviour of in situ AA8011-ZrB<sub>2</sub> metal matrix composites by using Taguchi-grey analysis," *Materials Science Forum*, vol. 928, pp. 162–167, 2018.
- [22] M. K. Sahu and R. K. Sahu, "Experimental investigation, modeling, and optimization of wear parameters of B<sub>4</sub>C and Fly-ash reinforced aluminum hybrid composite," *Frontiers of Physics*, vol. 8, p. 219, 2020.
- [23] G. Karthikeyan and G. Jinu, "Dry sliding wear behaviour of stir cast LM25/ZrO<sub>2</sub> metal matrix composites," *Transactions of Famena*, vol. 4, pp. 89–98, 2015.
- [24] C. Chanakyan, S. Sivasankar, M. Meignanamoorthy, and S. V. Alagarsamy, "Parametric optimization of mechanical properties via FSW on AA5052 using Taguchi based grey relational analysis," *Incas Bulletin*, vol. 13, no. 2, pp. 21–30, 2021.
- [25] P. Raveendran, S. V. Alagarsamy, M. Ravichandran, and M. Meignanamoorthy, "Effect of machining parameters on surface roughness for aluminium matrix composite by using Taguchi method with decision tree algorithm," *Surface Review and Letters*, vol. 28, no. 4, article 2150021, 2021.
- [26] S. V. Alagarsamy, M. Ravichandran, and H. Saravanan, "Development of mathematical model for predicting the electric erosion behaviour of TiO<sub>2</sub> filled Al-Zn-Mg-Cu (AA7075) alloy composite using RSM-DFA method," *Journal of Advanced Manufacturing Systems*, vol. 20, no. 1, pp. 1–26, 2021.
- [27] S. V. Alagarsamy and M. Ravichandran, "Investigations on tribological behaviour of AA7075-TiO<sub>2</sub> composites under dry sliding conditions," *Industrial Lubrication and Tribology*, vol. 71, pp. 1064–1071, 2019.
- [28] V. Mohanavel, S. Prasath, K. Yoganandam, B. G. Tesemma, and S. S. Kumar, "Optimization of wear parameters of aluminium composites (AA7150/10 wt%WC) employing Taguchi approach," *Materials Today: Proceedings*, vol. 33, pp. 4742–4745, 2020.